Orbital magneto-optical response of periodic insulators from first principles

Irina V. Lebedeva,[1,*] David A. Strubbe,[2] Ilya V. Tokatly,[1,3,4] and Angel Rubio[1,5,†]

[1] *Nano-Bio Spectroscopy Group and ETSF, Departamento de Física de Materiales, Universidad del País Vasco UPV/EHU- 20018 San Sebastián, Spain*

[2] *Department of Physics, School of Natural Sciences, University of California, Merced, CA 95343, United States*

[3] *Donostia International Physics Center (DIPC), Manuel de Lardizabal 5, 20018 San Sebastián, Spain*

[4] *IKERBASQUE, Basque Foundation for Science, 48011 Bilbao, Spain*

[5] *Max Planck Institute for the Structure and Dynamics of Matter and Center for Free-Electron Laser Science, Luruper Chaussee 149, 22761 Hamburg, Germany*

We present a reformulation of the density matrix perturbation theory for time-dependent electromagnetic fields under periodic boundary conditions, which allows us to treat the orbital magneto-optical response of solids at the *ab initio* level. The efficiency of the computational scheme proposed is comparable to standard linear-response calculations of absorption spectra and the results of tests for molecules and solids agree with the available experimental data. A clear signature of the valley Zeeman effect is revealed in the magneto-optical spectrum of a single layer of hexagonal boron nitride. The present formalism opens the path towards the study of magneto-optical effects in strongly driven low-dimensional systems.

Magneto-optical phenomena originating from the loss of symmetry between left (σ_+) and right (σ_-) circularly polarized light in the presence of a magnetic field are widely used for characterization of different kinds of matter [1, 2]. Magnetic circular dichroism (MCD) spectra help to assign overlapping bands and give insight into magnetic properties of the ground and excited states. Faraday rotation of the plane of polarization of linearly polarized light serves as a basic operational principle for functional magneto-optical disks and optical isolators [3]. Optical excitations in the presence of a magnetic field allow manipulation of valley pseudospin degrees of freedom in two-dimensional monolayers [4–10]. Giant Faraday rotation has been revealed in graphene [11] and metal oxide nanosheets [12]. Novel magneto-optical phenomena [13] are expected in recently discovered Z_2 topological insulators [14]. These advances cultivate the growing interest to development of a gauge-invariant and computationally efficient *ab initio* theory of magneto-optical response.

While *ab initio* calculations of MCD spectra in molecules can be performed nowadays in a nearly routine fashion [15–19] (as implemented in many quantum chemistry codes [20, 21]), the complete response theory for extended systems is still under development. The reason is that external electromagnetic fields break the translational symmetry of such systems, which in the formal way is expressed through unboundness of the position operator. Though according to the modern theory of polarization [22–24], the position operator can be replaced by a derivative with respect to the wave vector in responses to electric fields, the description of magnetic fields is more complicated as it introduces vector coupling to electron dynamics and leads to non-perturbative changes in wavefunctions. Three approaches have been considered in literature to deal with these difficulties: (1) taking a long-wavelength limit of an oscillating perturbation [25, 26], (2) using the Wannier function formalism [27–30] or (3) treating perturbations of the one-particle Green function or density matrix [30–32], which are two-point quantities summed up over all occupied bands and having gauge-invariant counterparts. While wave functions may change drastically in the presence of even a vanishing magnetic field, the gauge-invariant counterpart of the density matrix changes perturbatively [30–32]. We believe that using approach (3) helps to reduce numerical errors that may arise, for example, from summing up non-gauge-invariant paramagnetic and diamagnetic terms in approach (1). Approach (3) also allows us to work under purely periodic boundary conditions as opposed to approach (2), where contributions of open boundaries should be treated carefully [27–29].

So far the magnetic field has been considered in the context of static responses [25–32]. In the present letter we demonstrate that density matrix perturbation theory [30, 32, 33] can be straightforwardly extended to the case of dynamical non-linear phenomena. We focus on second-order magneto-optical effects, i.e. the change of the optical response in the presence of a magnetic field. While the approach developed here is general and can be adapted to any first-principles framework, we decide to illustrate it using time-dependent density functional theory (TDDFT) as this method provides a reasonable level of accuracy at a moderate computational cost. The implemented procedures form a part of the open-source code Octopus [34–36]. For the sake of simplicity, we limit our consideration to orbital magneto-optical effects for insulators. While the spin contribution is trivial, the account of the Fermi surface contribution can be done for metals by analogy with Ref. [26].

Let us consider the response to uniform magnetic and

electric fields. We use the temporal gauge, in which both of these fields are described by the vector potential $\mathbf{A}$ and are given by $\mathbf{B} = \nabla \times \mathbf{A}$ and $\mathbf{E} = -c^{-1}\partial_t \mathbf{A}$, respectively, where c is the speed of light (atomic units are used throughout the letter). Though the fields are uniform, the vector potential $\mathbf{A}$ entering in the Hamiltonian H is non-periodic. This gives rise to ill-defined expectation values of quantum mechanical operators describing physical properties of the system in the periodic basis. The operators are gauge-dependent but this non-periodicity cannot be resolved by changing the gauge. However, it turns out that for any operator $\mathcal{O}$ it is possible to distinguish the periodic and gauge-invariant counterpart $\tilde{\mathcal{O}}$ by factoring out the Aharonov-Bohm-type phase $\varphi_{12} = -c^{-1}\int_{\mathbf{r}_2}^{\mathbf{r}_1} \mathbf{A}(\mathbf{r})\mathrm{d}\mathbf{r}$ [30–32]

$$\mathcal{O}_{\mathbf{r}_1\mathbf{r}_2} = \tilde{\mathcal{O}}_{\mathbf{r}_1\mathbf{r}_2} \exp\left(i\varphi_{12}\right). \tag{1}$$

Here we take $\hbar = e = 1$ and the integral is taken along the straight line between points $\mathbf{r}_2$ and $\mathbf{r}_1$ so that $\mathbf{r} = \mathbf{r}_2 + (\mathbf{r}_1 - \mathbf{r}_2)\xi$, $0 \le \xi \le 1$. This approach was previously used to derive corrections to the gauge-invariant counterpart $\tilde{\rho}$ of the density matrix ρ in the static magnetic field [30–32]. In the present paper we generalize these derivations to the case of time-dependent electromagnetic fields by rewriting the exact time-dependent Liouville equation $-i\partial_t\rho + [H,\rho] = 0$ in terms of $\tilde{\rho}$:

$$\begin{aligned} &-i\left(\partial_t + i\partial_t\varphi_{13}\right)\tilde{\rho}_{\mathbf{r}_1\mathbf{r}_3} = \\ &\int d\mathbf{r}_2 e^{i\varphi_{123}}\left(\tilde{\rho}_{\mathbf{r}_1\mathbf{r}_2}\tilde{H}_{\mathbf{r}_2\mathbf{r}_3} - \tilde{H}_{\mathbf{r}_1\mathbf{r}_2}\tilde{\rho}_{\mathbf{r}_2\mathbf{r}_3}\right), \end{aligned} \tag{2}$$

where the phase φ_{123} on the right-hand side is given by the flux of the vector potential through the triangle formed by points $\mathbf{r}_1$, $\mathbf{r}_2$ and $\mathbf{r}_3$ so that $\varphi_{123} = \varphi_{12} + \varphi_{23} + \varphi_{31} = \mathbf{B}\cdot(\mathbf{r}_1 - \mathbf{r}_2)\times(\mathbf{r}_2 - \mathbf{r}_3)/2c$. The corresponding exponential term can be used to obtain corrections to the density matrix to any order in the magnetic field, while the time derivative of the phase φ_{13} on the left-hand side is responsible for linear change in the density matrix due to the electric field $\partial_t\varphi_{13} = \mathbf{E}\cdot(\mathbf{r}_1 - \mathbf{r}_3)$. It is seen, therefore, that Eq. (2) is gauge-invariant and includes all-order corrections to time-dependent electric and magnetic fields.

To describe the magneto-optical effects on the basis of Eq. (2) we assume that $\mathbf{E}$ corresponds to the oscillating electric field of the electromagnetic wave and $\mathbf{B}$ to the static magnetic field applied. The magnetic field of the electromagnetic wave is neglected. We, therefore, consider only the first-order corrections in $\mathbf{E}$, $\mathbf{B}$ and $\mathbf{E}\times\mathbf{B}$. Keeping only the terms to the first order in the magnetic field is reasonable even for strong magnetic fields $B \ll c/a^2 \sim 10^5$ T, where $a = 1$ Å is taken as a typical interatomic distance. The equation for the density response then takes the form

$$-i\partial_t\tilde{\rho} + [\tilde{H},\tilde{\rho}] = -\frac{1}{2}\left\{\mathbf{E} + \frac{1}{c}\mathbf{V}\times\mathbf{B}, [\mathbf{r},\tilde{\rho}]\right\}, \tag{3}$$

where $\tilde{O}_{\mathbf{r}_1\mathbf{r}_2}(\mathbf{r}_1 - \mathbf{r}_2) = [\mathbf{r},\tilde{O}]_{\mathbf{r}_1\mathbf{r}_2}$, $\tilde{H}$ can be different from the unperturbed Hamiltonian H_0 due to local-field effects, i.e. self-consistent variation of Hartree and exchange-correlation potentials upon changes in the electron density, $\mathbf{V} = -i[\mathbf{r},\tilde{H}]$ is the velocity operator computed with account of all non-local contributions to the Hamiltonian, such as from non-local pseudopotentials, and the scalar product is assumed between the operators entering into the anticommutator on the right-hand side. This is simply the quantum Bolzmann equation with the Lorentz driving force. Unlike the singular position operator $\mathbf{r}$, the commutator $[\mathbf{r},\tilde{\rho}]$ of the position operator with the periodic function $\tilde{\rho}$ is well defined here and can be substituted by the derivative with respect to the wave vector, $i\partial_{\mathbf{k}}\rho_{\mathbf{k}}$, in reciprocal space [30–32]. Differentiating the Liouville equation (3), one can evaluate the derivatives of the density matrix $\tilde{\rho}^{(P)} = \partial\tilde{\rho}/\partial P$ with respect to perturbations P of parameters of the Hamiltonian, such as the electric field $\mathbf{E}$ or magnetic field $\mathbf{B}$.

Following the density-matrix perturbation theory [33], we project the Liouville equation (3) onto unperturbed wavefunctions $|\psi^{(0)}_{v\mathbf{k}}\rangle$ of occupied bands v and find its solution $|\eta^{(P)}_{v\mathbf{k}}(\Omega)\rangle = P_c\tilde{\rho}^{(P)}(\Omega)|\psi^{(0)}_{v\mathbf{k}}\rangle$ within the unoccupied subspace according to the Sternheimer approach [36–38] (see Supplementary Information). Here $P_c = 1 - P_v = 1 - \rho^{(0)}$ is the projector on the unoccupied bands, and $\Omega = \Omega_0 + i\delta$ is frequency considered, where Ω_0 is the frequency of the external perturbation and $i\delta$ is the small but finite imaginary frequency added to avoid divergences at resonances [36–39]. Then elements of derivatives of the density matrix between unoccupied (C subscript) and occupied (V subscript) subspaces are computed as $\tilde{\rho}^{(P)}_{\mathrm{CV}}(\Omega) = \int_{\mathrm{BZ}}(2\pi)^{-3}d\mathbf{k}\sum_v |\eta^{(P)}_{v\mathbf{k}}(\Omega)\rangle\langle\psi^{(0)}_{v\mathbf{k}}|$ and $\tilde{\rho}^{(P)}_{\mathrm{VC}}(\Omega) = (\tilde{\rho}^{(P)}_{\mathrm{CV}}(-\Omega^*))^*$. The block diagonal elements $\tilde{\rho}^{(P)}_{\mathrm{D}}$ of derivatives to the density matrix within occupied ($\tilde{\rho}^{(P)}_{\mathrm{VV}} = -P_v\tilde{\rho}^{(P)}_{\mathrm{D}}P_v$) and unoccupied ($\tilde{\rho}^{(P)}_{\mathrm{CC}} = P_c\tilde{\rho}^{(P)}_{\mathrm{D}}P_c$) subspaces are calculated from the idempotency condition for the full density matrix $\rho = \rho\rho$, which in terms of its periodic counterpart $\tilde{\rho}$ and to the first order in the magnetic field is given by [30, 32]

$$\tilde{\rho} = \tilde{\rho}\tilde{\rho} + \frac{i}{2c}\mathbf{B}\cdot[\mathbf{r},\tilde{\rho}]\times[\mathbf{r},\tilde{\rho}] \tag{4}$$

The commutator $[\mathbf{r},\tilde{\rho}]$ corresponding to $i\partial_{\mathbf{k}}\tilde{\rho}_{\mathbf{k}}$ in reciprocal space is calculated within the $\mathbf{k}\cdot\mathbf{p}$ theory [36–38] (see Supplementary Information).

The contribution $\alpha_{\nu\mu,\gamma}$ to the polarizability in the presence of the magnetic field ($\alpha_{\nu\mu} = \alpha_{0\nu\mu} + \alpha_{\nu\mu,\gamma}B_\gamma$) is obtained from the current response as

$$\alpha_{\nu\mu,\gamma}(\Omega) = \frac{i}{\Omega}\mathrm{Tr}\left[V_\nu\tilde{\rho}^{(E_\mu B_\gamma)}(\Omega)\right]. \tag{5}$$

MCD response is measured as the ellipticity ξ_z gained by the linearly polarized light transmitted along the z

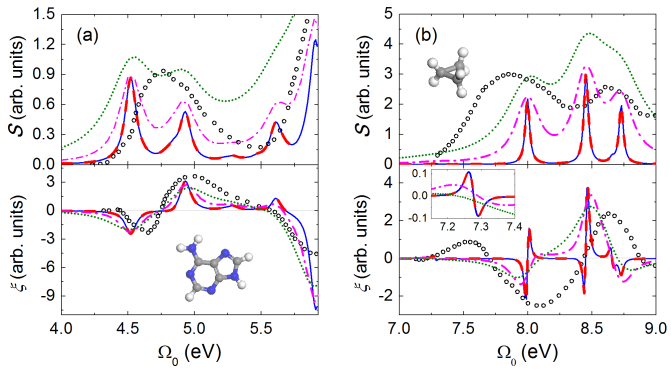

FIG. 1. (Colour online) Absorption cross-section S and ellipticity ξ (in arbitrary units) for (a) adenine ($\delta = 0.05$ eV) and (b) cyclopropane ($\delta = 0.02$ eV) as functions of the frequency of light Ω_0 (in eV) calculated using the present solid-state formalism (solid blue lines) and standard finite-system formulation (red dashed lines). The corresponding curves are virtually indistinguishable. The results obtained in the finite-system formulation for linewidths $\delta = 0.1$ eV and $\delta = 0.2$ eV are shown by magenta dash-dotted lines and green dotted lines, respectively. The experimental data for adenine [40] in water and cyclopropane [41] in the gas phase are represented by circles. The parts of the spectra shown lie below the ionization potential at zero temperature (6.7 eV and 9.4 eV for adenine and cyclopropane, respectively). Carbon, hydrogen and nitrogen atoms in the atomistic structures are coloured in medium gray, white and blue/dark gray, respectively. The inset shows the first MCD peak of cyclopropane.

axis per unit length, which comes from the difference in $\sigma_\pm$ absorption and is given by [1]

$$\xi_z(\Omega_0) = \frac{\pi\Omega_0}{wc} B_z \mathrm{Re}\left[\frac{\alpha_{xy,z}(\Omega) - \alpha_{yx,z}(\Omega)}{n_0}\right], \quad (6)$$

where n_0 is the refractive index and w is the volume per molecule or volume of the unit cell for solids. The angle of Faraday rotation is determined by a similar expression but with the imaginary part of $\alpha_{\nu\mu,\gamma}$ instead of the real one. By contrast, in the magneto-optical polar Kerr effect for reflected light, the ellipticity and angle of rotation are determined by Im $\alpha_{\nu\mu,\gamma}$ and Re $\alpha_{\nu\mu,\gamma}$, respectively [2].

The new formalism for calculation of the magneto-optical response has been implemented in the Octopus code [34–36] and first tested for molecules (Fig. 1) in a large simulation box with periodic boundary conditions. The orientationally averaged ellipticity is given by $\xi = \sum_\gamma \xi_\gamma/3$. The absorption cross-section is computed as $S = 4\pi\Omega_0 \mathrm{Im}\ \alpha_{0\nu\nu}/(3c)$ [35, 36], where the polarizability $\alpha_{0\nu\mu}$ is found using $\tilde{\rho}^{(E_\mu)}$ instead of $\tilde{\rho}^{(E_\mu B_\gamma)}$ in Eq. (5). The interaction of valence electrons with atomic cores is described using Troullier-Martins norm-conserving pseudopotentials [42]. The local-density approximation (LDA) [43] is applied for the ground state and the adiabatic LDA kernel for the response (though the theory could be equally used with other functionals). The density-averaged self-interaction correction [44] is used to avoid spurious transitions to diffuse excited states. Only the Γ point is considered. The size of the simulation box of 24 Å and the spacing of the real-space grid of 0.14 Å are sufficient for convergence of the magneto-optical spectra.

The calculations for cyclopropane and adenine (Fig. 1) reveal that the present formalism gives the results indistinguishable from the formulation using the position operator $\mathbf{r}$ (see Supplementary Information), which is commonly applied in literature for finite systems [15–19], and in agreement with the experimental data [40, 41]. MCD response of molecules can be divided into $\mathcal{A}$ and $\mathcal{B}$ terms. The $\mathcal{B}$ [15, 17, 18] comes from perturbations of molecular states in the magnetic field and is present in all systems. The $\mathcal{A}$ term [15, 17, 19] comes from perturbations of energies of excited states with non-zero orbital angular momenta. Such states are present only in molecules with rotational symmetry at least of the third order like cyclopropane. Since transitions to states with opposite orbital angular momenta are coupled to the light of different polarization, Zeeman splitting leads to an energy shift between $\sigma_\pm$ absorption peaks. MCD response, i.e. the difference in $\sigma_\pm$ absorption, in this case is described by the derivative of the spectral density [18, 19] and has second-order poles. The $\mathcal{A}$ term is clearly dominant for cyclopropane at linewidth $\delta = 0.02$ eV (Fig. 1b), in agreement with previous calculations [15]. Raising the linewidth to the experimental values $\delta = 0.1 - 0.2$ eV decreases the $\mathcal{A}$ term relative to the $\mathcal{B}$ term and brings the shape of the calculated curve closer to the experimental one. After this, the changes in the sign of the MCD signal are described well not only for adenine (Fig. 1a) but also for cyclopropane (Fig. 1b).

To test the developed formalism for solids we have applied it to bulk silicon and a monolayer of hexagonal boron nitride. The dielectric tensor is computed as $\epsilon_{\nu\mu} = \delta_{\nu\mu} + 4\pi\alpha_{\nu\mu}/w$. While account of local-field effects is very important for molecules, for the solids considered, these effects provide a minor correction to the spectra (see the example for boron nitride in Supplementary Information) and are not included below. The linewidth $\delta = 0.1$ eV is used. For boron nitride, we consider the rectangular unit cell of 4.294 Å × 2.479 Å × 24.0 Å with four atoms. For silicon, the cubic unit cell of 5.38 Å size with 8 atoms is studied and the grid spacing is increased to 0.25 Å. Integration over the Brillouin zone is performed according to the Monkhorst-Pack method [49]. 3000 irreducible k-points are needed for convergence for boron nitride and 6600 for silicon (see Supplementary Information).

The data computed for bulk silicon follow the shape of the experimental curves [2] for Re ϵ_{xy} and Im ϵ_{xy} at the direct absorption edge (Fig. 2a). The analysis of optical transitions at the Γ point of the Brillouin zone, where the highest valence and lowest conduction bands are formed by triply degenerate p-like states (Γ'_{25} and Γ_{15}, respec-

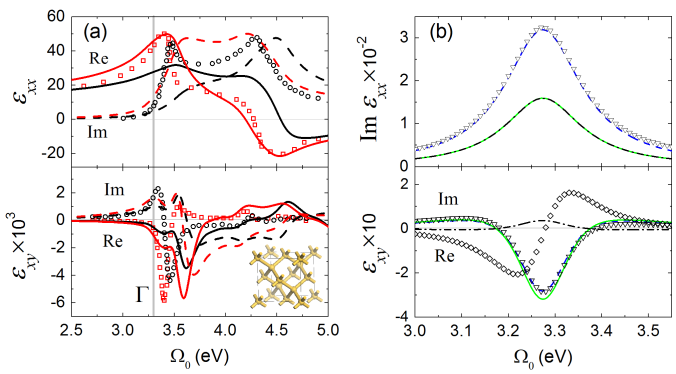

FIG. 2. (Colour online) (a) Calculated components ϵ_{xx} (upper panel) and ϵ_{xy} (lower panel) of the dielectric tensor for silicon as functions of the frequency of light Ω_0 (in eV) for the magnetic field of 1 T along the z axis. The real and imaginary parts are shown by solid and dashed lines, respectively. The results obtained in the independent-particle approximation and using the LRC kernel correspond to black and red/gray lines, respectively. The calculated data are blue-shifted in energy by 0.7 eV to take into account the GW correction to the band gap [45, 46]. The experimental data from Refs. [47] and [2] for ϵ_{xx} and ϵ_{xy} (scaled by a factor of 1/3), respectively, are shown by symbols. Squares correspond to the real parts and circles to the imaginary ones. The transitions at the Γ point of the Brillouin zone are indicated by the vertical gray line. (b) Calculated contributions to Im ϵ_{xx} (upper panel) and Im ϵ_{xy} (lower panel) from the Γ point: total contribution (triangles), contribution from transitions $\Gamma'_{25} \to \Gamma_{15}$ to the $\mathcal{A}$ term (blue dashed lines) and contributions from transitions $\Gamma'_{25} \to \Gamma_{15}$ with the magnetic quantum number $l_z = 0 \to \pm 1$ (green solid lines) and $\pm 1 \to 0$ (black dash-dotted lines) to the $\mathcal{A}$ term. Total Re ϵ_{xy} is shown by diamonds.

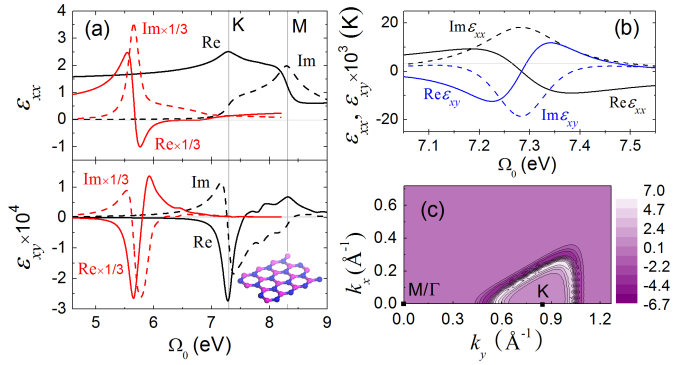

FIG. 3. (Colour online) (a) Calculated components ϵ_{xx} (upper panel) and ϵ_{xy} (lower panel) of the dielectric tensor for a boron nitride monolayer as functions of the frequency of light Ω_0 (in eV) for the magnetic field of 1 T along the z axis directed out of the plane. The real and imaginary parts are represented by solid and dashed lines, respectively. The results obtained in the independent-particle approximation and using the LRC kernel (multiplied by a factor of 1/3) are shown by black and red/gray lines, respectively. The calculated data are blue-shifted in energy by 2.6 eV to take into account the GW correction to the band gap [48]. The results obtained with the LRC kernel are additionally red-shifted by 1.4 eV to account for the binding energy of the first exciton [48]. The transitions at the K and M points of the Brillouin zone are indicated by vertical gray lines. Boron and nitrogen atoms in the atomistic structure are coloured in magenta/medium gray and blue/dark gray, respectively. (c) Calculated contributions to ϵ_{xx} (black lines) and ϵ_{xy} (blue/gray lines) from the K points of the Brillouin zone. (d) Calculated contributions to Re $\epsilon_{xy} \times 10^3$ from different points (k_x,k_y,0) (in Å^{-1}) of the Brillouin zone of the 4-atom cell for $\Omega_0 = 7.8$ eV.

tively) [50], reveals significant contributions that can be attributed to the $\mathcal{A}$ term (Fig. 2b). Two inequivalent contributions come from excitations with the change in the magnetic quantum number l_z from 0 to ±1 and vice versa. The ratio $\epsilon_{xy}/\epsilon_{xx}$ for each of them at the resonance frequency characterizes the relative frequency shift in the magnetic field $\epsilon_{xy}/\epsilon_{xx} \sim \Delta m_z B_z \Delta l_z/\delta$, where Δm_z is the change in the orbital magnetic dipole moment (see Supplementary Information). The corresponding effective g-factors $g = -\Delta m_z/\mu_B \Delta l_z$, where μ_B is the Bohr magneton, are $g = 3.5$ in $\Gamma'_{25} \to \Gamma_{15}$ transitons with $l_z = 0 \to \pm 1$ and only $g = -0.40$ for $l_z = \pm 1 \to 0$. Thus, unlike absorption, transitions $l_z = 0 \to \pm 1$ prevail in the magneto-optical response at the band edge. The domination of the $\mathcal{A}$ term is consistent with the experiments, where Re/Im ϵ_{xy} look similar to derivatives of Im/Re ϵ_{xx} (Fig. 2a). The agreement with the experimental data is further improved when we model excitonic effects using the long-range contribution (LRC) to the exchange-correlation kernel $f_{xc}^{(\mathrm{LRC})}(\mathbf{q}) = -\beta/q^2$ with $\beta = 0.2$ in reciprocal space [45, 46, 51].

In boron nitride, the magneto-optical response of continuum states starts from a prominent peak at the band edge even without account of excitonic effects (Fig. 3a). In this material, the first optical transitions take place at the $K^{\pm}$ points in the corners of the hexagonal Brillouin zone, where phase winding of wavefunctions related to the C_3 symmetry imposes coupling to only one ($\sigma_{\pm}$) light component [52–54]. The magneto-optical response from the $K^{\pm}$ points is just a second-order pole (Fig. 3b). The domination of the $\mathcal{A}$ term is also seen from the map for different k-points (Fig. 3c). Clearly the response of boron nitride at the band edge is related to the valley Zeeman effect [4–9]. Since the density of states in two-dimensional materials tends to the Heaviside step function in the limit of zero linewidth, the $\mathcal{A}$ term related to its derivative approaches a delta peak. Therefore, discrete peaks in continuum magneto-optical spectra of two-dimensional materials are indicators of the Zeeman splitting.

The change of the magnetic dipole moment upon the excitation at the $K^{\pm}$ points is $\Delta m_z^{\pm} \approx \mp 1.8 \mu_B$. Explicit calculations of the magnetic dipole moments according to [26, 55] give $\mp 0.95 \mu_B$ and $\mp 2.8 \mu_B$ for the valence and conduction bands, respectively. The calculated valley g-factor $g^{\mathrm{vl}} = -2\Delta m_z^{+}/\mu_B = 3.6$ is, thus, close to the

magnitudes of g-factors of about 4 in photoluminescence experiments for WSe_2 [4–7] and $MoSe_2$ [7–9] monolayers.

It is known, however, that boron nitride exhibits strong excitonic effects [48]. To mimic the first bound exciton we apply the LRC kernel [45, 46, 51] with $\beta = 10$ (Fig. 3a). Using the kernel, the spectra become more similar to those of symmetric molecules like cyclopropane (Fig. 1b).

The efficiency of the implemented procedures for magneto-optics is comparable to standard linear-response calculations of polarizability in the absence of the magnetic field. When local-field effects are included, magneto-optics for solids takes only twice as long as polarizability (due to the need for response at $\Omega_0 \pm i\delta$, see Supplementary Information). Although the LDA functional is used here for testing purposes, nothing impedes using more accurate hybrid functionals or translating the same approach into the many-body framework.

We acknowledge the financial support from the European Research Council (ERC-2015-AdG-694097), Grupos Consolidados (IT578-13), European Union's H2020 program under GA no. 646259 (MOSTOPHOS) and no. 676580 (NOMAD) and Spanish Ministry (MINECO) Grant No. FIS2016-79464-P.

REFERENCES

* liv_ira@hotmail.com
† angel.rubio@mpsd.mpg.de

[1] L. D. Barron, *Molecular Light Scattering and Optical Activity*, 2nd ed. (Cambridge University Press, Cambridge, 2004).
[2] F. R. Keßler and J. Metzdorf, in *Modern Problems in Condensed Matter Sciences*, Vol. 27.1, edited by V. M. Agranovich and A. A. Maradudin (Elsevier Science Publishers, Amsterdam, 1991) Chap. 11.
[3] S. Sugano and N. Kojima, eds., *Magneto-optics* (Springer, Berlin, 1999).
[4] A. Srivastava, M. Sidler, A. V. Allain, D. S. Lembke, A. Kis, and A. Imamoğlu, Nat. Phys. **11**, 141 (2015).
[5] G. Aivazian, Z. Gong, A. M. Jones, R.-L. Chu, J. Yan, D. G. Mandrus, C. Zhang, D. Cobden, W. Yao, and X. Xu, Nat. Phys. **11**, 148 (2015).
[6] A. A. Mitioglu, P. Plochocka, A. Granados del Aguila, P. C. M. Christianen, G. Deligeorgis, S. Anghel, L. Kulyuk, and D. K. Maude, Nano Lett. **15**, 4387 (2015).
[7] G. Wang, L. Bouet, M. M. Glazov, T. Amand, E. L. Ivchenko, E. Palleau, X. Marie, and B. Urbaszek, 2D Materials **2**, 034002 (2015).
[8] D. MacNeill, C. Heikes, K. F. Mak, Z. Anderson, A. Kormányos, V. Zólyomi, J. Park, and D. C. Ralph, Phys. Rev. Lett. **114**, 037401 (2015).
[9] Y. Li, J. Ludwig, T. Low, A. Chernikov, X. Cui, G. Arefe, Y. D. Kim, A. M. van der Zande, A. Rigosi, H. M. Hill, S. H. Kim, J. Hone, Z. Li, D. Smirnov, and T. F. Heinz, Phys. Rev. Lett. **113**, 266804 (2014).
[10] C. J. Tabert and E. J. Nicol, Phys. Rev. Lett. **110**, 197402 (2013).
[11] I. Crassee, J. Levallois, A. L. Walter, M. Ostler, A. Bostwick, E. Rotenberg, T. Seyller, D. van der Marel, and A. B. Kuzmenko, Nat. Phys. **7**, 48 (2011).
[12] M. Osada, Y. Ebina, K. Takada, and T. Sasaki, Adv. Mater. **18**, 295 (2006).
[13] W.-K. Tse and A. H. MacDonald, Phys. Rev. B **82**, 161104 (2010).
[14] X.-L. Qi, T. L. Hughes, and S. C. Zhang, Phys. Rev. B **78**, 195424 (2008).
[15] H. Solheim, K. Ruud, S. Coriani, and P. Norman, J. Chem. Phys. **128**, 094103 (2008).
[16] H. Solheim, K. Ruud, S. Coriani, and P. Norman, J. Phys. Chem. A **112**, 9615 (2008).
[17] K.-M. Lee, K. Yabana, and G. F. Bertsch, J. Chem. Phys. **134**, 144106 (2011).
[18] M. Seth, M. Krykunov, T. Ziegler, J. Autschbach, and A. Banerjee, J. Chem. Phys. **128**, 144105 (2008).
[19] M. Seth, M. Krykunov, T. Ziegler, and J. Autschbach, J. Chem. Phys. **128**, 234102 (2008).
[20] K. Aidas, C. Angeli, K. L. Bak, V. Bakken, R. Bast, L. Boman, O. Christiansen, R. Cimiraglia, S. Coriani, P. Dahle, E. K. Dalskov, U. Ekström, T. Enevoldsen, P. Eriksen, J. J.and Ettenhuber, B. Fernández, L. Ferrighi, H. Fliegl, L. Frediani, K. Hald, A. Halkier, C. Hättig, H. Heiberg, T. Helgaker, A. C. Hennum, H. Hettema, E. Hjertenæs, S. Høst, I. Høyvik, B. Iozzi, M. F.and Jansík, H. J. Jensen, D. Jonsson, P. Jørgensen, J. Kauczor, S. Kirpekar, T. Kjærgaard, W. Klopper, S. Knecht, R. Kobayashi, H. Koch, J. Kongsted, A. Krapp, K. Kristensen, A. Ligabue, O. B. Lutnæs, J. I. Melo, K. V. Mikkelsen, R. H. Myhre, C. Neiss, C. B. Nielsen, P. Norman, J. Olsen, J. M. Olsen, A. Osted, M. J. Packer, F. Pawlowski, T. B. Pedersen, P. F. Provasi, S. Reine, Z. Rinkevicius, T. A. Ruden, K. Ruud, V. V. Rybkin, P. Sałlek, C. C. Samson, A. S. de Merás, T. Saue, S. P. Sauer, B. Schimmelpfennig, K. Sneskov, A. H. Steindal, K. O. Sylvester-Hvid, P. R. Taylor, A. M. Teale, E. I. Tellgren, D. P. Tew, A. J. Thorvaldsen, L. Thøgersen, O. Vahtras, M. A. Watson, D. J. Wilson, M. Ziolkowski, and H. Ågren, WIREs: Comput. Mol. Sci. **4**, 269 (2013).
[21] G. te Velde, F. M. Bickelhaupt, E. J. Baerends, C. Fonseca Guerra, S. J. A. van Gisbergen, J. G. Snijders, and T. Ziegler, J. Comput. Chem. **22**, 931 (2001).
[22] R. D. King-Smith and D. Vanderbilt, Phys. Rev. B **47**, 1651 (1993).
[23] D. Vanderbilt and R. D. King-Smith, Phys. Rev. B **48**, 4442 (1993).
[24] R. Resta, Rev. Mod. Phys. **66**, 899 (1994).
[25] F. Mauri and S. G. Louie, Phys. Rev. Lett. **76**, 4246 (1996).
[26] J. Shi, G. Vignale, D. Xiao, and Q. Niu, Phys. Rev. Lett. **99**, 197202 (2007).
[27] T. Thonhauser, D. Ceresoli, D. Vanderbilt, and R. Resta, Phys. Rev. Lett. **95**, 137205 (2005).
[28] D. Ceresoli, T. Thonhauser, D. Vanderbilt, and R. Resta, Phys. Rev. B **74**, 024408 (2006).
[29] A. Malashevich, I. Souza, S. Coh, and D. Vanderbilt, New J. Phys. **12**, 053032 (2010).
[30] A. M. Essin, A. M. Turner, J. E. Moore, and D. Vanderbilt, Phys. Rev. B **81**, 205104 (2010).

[31] K.-T. Chen and P. A. Lee, Phys. Rev. B **84**, 205137 (2011).

[32] X. Gonze and J. W. Zwanziger, Phys. Rev. B **84**, 064445 (2011).

[33] M. Lazzeri and F. Mauri, Phys. Rev. B **68**, 161101 (2003).

[34] M. A. L. Marques, A. Castro, G. F. Bertsch, and A. Rubio, Comput. Phys. Commun. **151**, 60 (2003).

[35] A. Castro, H. Appel, M. Oliveira, C. A. Rozzi, X. Andrade, F. Lorenzen, M. A. L. Marques, E. K. U. Gross, and A. Rubio, Phys. Status Solidi B **243**, 2465 (2006).

[36] X. Andrade, D. A. Strubbe, U. De Giovannini, A. H. Larsen, M. J. T. Oliveira, J. Alberdi-Rodriguez, A. Varas, I. Theophilou, N. Helbig, M. J. Verstraete, L. Stella, F. Nogueira, A. Aspuru-Guzik, A. Castro, M. A. L. Marques, and A. Rubio, Phys. Chem. Chem. Phys. **17**, 31371 (2015).

[37] D. A. Strubbe, *Optical and transport properties of organic molecules: Methods and applications* (PhD thesis, University of California, Berkeley, USA, 2012).

[38] D. A. Strubbe, L. Lehtovaara, A. Rubio, M. A. L. Marques, and S. G. Louie, "Response functions in TDDFT: Concepts and implementation," in *Fundamentals of Time-Dependent Density Functional Theory*, edited by M. A. Marques, N. T. Maitra, F. M. Nogueira, E. Gross, and A. Rubio (Springer Berlin Heidelberg, Berlin, Heidelberg, 2012) pp. 139–166.

[39] X. Andrade, S. Botti, M. A. L. Marques, and A. Rubio, J. Chem. Phys. **126**, 184106 (2007).

[40] J. C. Sutherland and K. Griffin, Biopolymers **23**, 2715 (1984).

[41] A. Gedanken and O. Schnepp, Chem. Phys. **12**, 341 (1976).

[42] N. Troullier and J. L. Martins, Phys. Rev. B **43**, 1993 (1991).

[43] J. P. Perdew and A. Zunger, Phys. Rev. B **23**, 5048 (1981).

[44] C. Legrand, E. Suraud, and P.-G. Reinhard, J. Phys. B At. Mol. Opt. Phys. **35**, 1115 (2002).

[45] S. Albrecht, L. Reining, R. Del Sole, and G. Onida, Phys. Rev. Lett. **80**, 4510 (1998).

[46] S. Botti, F. Sottile, N. Vast, V. Olevano, L. Reining, H.-C. Weissker, A. Rubio, G. Onida, R. Del Sole, and R. W. Godby, Phys. Rev. B **69**, 155112 (2004).

[47] P. Lautenschlager, M. Garriga, L. Viña, and M. Cardona, Phys. Rev. B **36**, 4821 (1987).

[48] L. Wirtz, A. Marini, and A. Rubio, AIP Conf. Proc. **786**, 391 (2005).

[49] H. J. Monkhorst and J. D. Pack, Phys. Rev. B **13**, 5188 (1976).

[50] M. Cardona and F. H. Pollak, Phys. Rev. **142**, 530 (1966).

[51] R. Stubner, I. V. Tokatly, and O. Pankratov, Phys. Rev. B **70**, 245119 (2004).

[52] W. Yao, D. Xiao, and Q. Niu, Phys. Rev. B **77**, 235406 (2008).

[53] T. Cao, G. Wang, W. Han, H. Ye, C. Zhu, J. Shi, Q. Niu, P. Tan, E. Wang, B. Liu, and J. Feng, Nat. Commun. **3**, 887 (2012).

[54] D. Xiao, G.-B. Liu, W. Feng, X. Xu, and W. Yao, Phys. Rev. Lett. **108**, 196802 (2012).

[55] M.-C. Chang and Q. Niu, Phys. Rev. B **53**, 7010 (1996).